Nucleon Loop as a Force in the $\pi\pi$ Channel*

Fritz Gutbrod

Deutsches Elektronen-Synchrotron DESY, Hamburg, Germany

(Received 17 July 1972)

The ρ meson is described as a $\pi\pi$-$N\bar{N}$ composite system, with N exchange as a nondiagonal force between the two channels. The resulting nucleon loop, as a force in the $\pi\pi$ channel, gives far too strong attraction, if calculated with unmodified nucleon propagators. The necessary cutoff parameter in the nucleon propagators is compared with the same quantity obtained in the $\Delta(1236)$ channel. Pion self-energy effects are introduced to improve the resulting ρ width, and crossing properties of the $\pi\pi$ p waves are discussed.

I. INTRODUCTION

For many purposes a composite picture of an elementary particle like the ρ meson may be useful, especially for an understanding of production processes and electromagnetic properties like form factors, etc. This is true even if we are not able to predict the mass and width of the particle with good accuracy. The most popular models for the ρ meson are first the $\pi\pi$ model[1] in which the wave function of the ρ meson is assumed to be dominated by the two-pion state; second, the quark model,[2] which is characterized by assuming a fermion-antifermion s-wave state to be the most important one, in strong similarity to the third picture, the Fermi-Yang model,[3] where the nucleon-antinucleon state is the favored one.

In none of these models are the necessary binding forces between the constituents understood quantitatively, and the assumption of vector-meson exchange as the dominant attractive force leads to a complicated bootstrap picture. Also the coupling between the above-mentioned channels, which is very strong, has rarely been taken into account. In this paper we want to pursue the idea, as an extreme point of view, that a synthesis between the $\pi\pi$ model and the Fermi-Yang model might be a realistic picture. We shall neglect direct interactions (e.g., ρ and ω exchange, respectively) in both the $\pi\pi$ and the $N\bar{N}$ channel and assume that the coupling between these channels proceeds through the simplest diagram possible, i.e., one-nucleon exchange. Consequently we may say that the interaction in the $\pi\pi$ channel is given by the baryon loop of Fig. 1(a) or, looking into the $N\bar{N}$ channel, that the attraction is due to the annihilation process of Fig. 1(b). This "force" in the $N\bar{N}$ system is attractive, in agreement with the general expectation that in the coupling to inelastic channels the positive definite contribution from the right-hand (physical) cut above the inelastic threshold of a partial-

wave amplitude dominates for diagrams like 1(b). This is to be compared with the strong attraction provided by t-channel ω and σ exchange in the Fermi-Yang model,[3] and it should be noted that diagram 1(b) can be read in the $N\bar{N}$ t channel as $N\bar{N}$ exchange with pion-exchange interaction. Thus the two pictures of mainly t-channel meson exchange in the $N\bar{N}$ system and of dominance of "annihilation" forces in the $N\bar{N}$ s channel are not necessarily inconsistent.

Our technical tool for solving this coupled channel problem will be the Bethe-Salpeter equation[4] for the $\pi\pi$ amplitude, with diagram 1(a) as the force term.

We do not expect that the nucleon loop, calculated strictly in fourth-order pseudoscalar perturbation theory, is a realistic two-pion irreducible amplitude, although its p-wave projection is not divergent. The experience with the nucleon exchange force in the $\Delta(1236)$ channel[5,6] in the ladder approximation tells us that the bare one-nucleon force is too strong, and a cutoff with a mass in the order of 2 GeV is necessary to suppress the short-range part of the "potential" such that we obtain the correct resonance energy in that model. If our picture for the Δ is reasonable, the cutoff in the nucleon loop of Fig. 1(a) necessary to generate the ρ meson with a mass of 760 MeV should be the same as in the Δ problem. This will turn out to be the case within 30%.

With this potential, however, we shall not be able to explain the width of the ρ meson, as the theoretical width exceeds the experimental one by more than a factor of 3. There are two possible ways to overcome this defect. First of all we can couple a third channel like $K\bar{K}$ or $\pi\omega$ to the $\pi\pi$ and $N\bar{N}$ channel, reducing the cutoff mass in the nucleon loop correspondingly and thereby the $\pi\pi$ interaction which controls the width. For convenience, however, we shall choose the $2N\bar{N}$ channel, coupled to the other states by the self-energy dia-
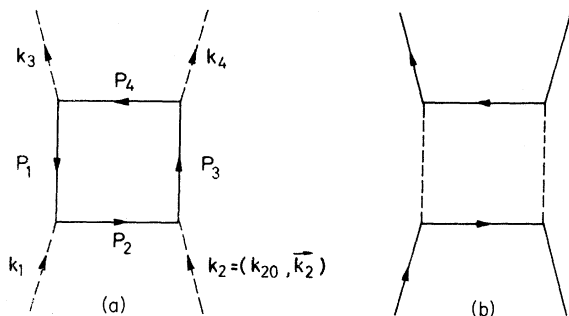
FIG. 1. (a) Baryon loop as a force in the $\pi\pi$ channel; (b) annihilation diagram as a force in the $N\bar{N}$ channel.

grams shown in Fig. 2. The effective coupling constant, needed to correct the width, exceeds the perturbation-theoretic value by a factor of 2. The second possibility would be to look for corrections within the nucleon loop which might increase the energy dependence of the potential, which trivially would lead to a narrower resonance. This has not been attempted here.

Our model has the virtue that, considering the $\pi\pi$ channel, the input force Fig. 1(a) is completely crossing symmetric. Solving the Bethe-Salpeter equation with this kernel of course destroys crossing symmetry, but we can now ask whether the neglected ladders in the t and u channels are important compared to the box diagram. This is not the case if we are concentrating on those kinematical regions where the potential is most important, namely where the off-shell mesons have four-momenta $k_i^2 (i=1,\ldots,4)$ of the order of $k_i^2 \lesssim -2M^2$. [M = nucleon mass. See Fig. 1(a) for kinematics.] Thus the gross properties of the ρ are probably not much influenced by ρ exchange.

In Sec. II we set up the Bethe-Salpeter equation and calculate its kernel. In Sec. III we discuss the results with a cutoff for the nucleon propagators and compare them with the $\Delta(1236)$ problem. In Sec. IV the modifications due to self-energy insertions are shown, and in Sec. V we investigate the crossing properties in detail. Section VI contains a summary and discussion, and in the Appendix the numerical details like integration techniques are explained.

II. BARYON LOOP AND THE BETHE-SALPETER EQUATION

In the notation of Bjorken and Drell[7] the contribution of the diagrams of Fig. 3(a) to the invariant $\pi\pi$ amplitude $M(k_1, k_2, k_3, k_4)$ or for short $M(k_i)$ is given by (the metric is + − − −)
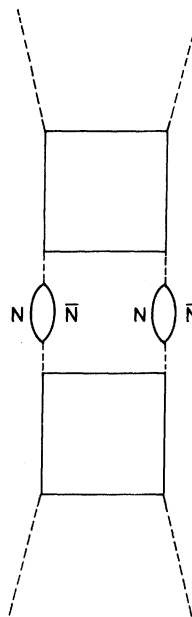
FIG. 2. Pion self-energy insertions as third coupled channel for the ρ meson.

$$M^{\text{loop}}(k_i) = -\left(\frac{g^2}{4\pi}\right)^2 \frac{4}{\pi^2}(\phi_1 \cdot \phi_2\phi_3^* \cdot \phi_4^* + \phi_1 \cdot \phi_3^*\phi_2 \cdot \phi_4^*$$

$$- \phi_1 \cdot \phi_4^*\phi_2 \cdot \phi_3^*)K(ki), \quad (1)$$

with

$$K(k_i) = i \int d^4q \frac{\text{tr}[(\not{P}_1 - M)(\not{P}_2 + M)(\not{P}_3 - M)(\not{P}_4 + M)]}{\prod_{i=1}^{4}(P_i^2 - M^2)},$$

$$(2)$$

$$\frac{g^2}{4\pi} = 14.5,$$

M = nucleon mass,

$$q = \tfrac{1}{2}(P_1 + P_3).$$

The momenta k_i and P_i are explained in Fig. 1(a), and ϕ_i are the isospin wave functions of the pions. The contribution to the isospin $I = 1$ channel is given by[7]

$$M_1^{\text{loop}}(k_i) = -\left(\frac{g^2}{4\pi}\right)^2 \frac{8}{\pi^2} K(k_i). \quad (3)$$

The diagrams of Fig. 3(b) do not contribute to the $I = 1$ state, whereas the $t \rightarrow u$ crossed diagrams of Fig. 3(c), which have the same p wave part as 3(a), should not be included in the kernel, since their iteration leads to the same diagrams obtained by iterating 3(a) except for a possible crossing of the external pions. They are omitted, and $t \rightarrow u$ crossing gives a factor of 2 in the final amplitude.

The sum of the s-channel iterated loop diagrams is given by the solution of the Bethe-Salpeter equation (BSE)

$$M_1(k_i) = M_1^{\text{loop}}(k_i)$$

$$-\frac{1}{i} \int \frac{d^4q}{(2\pi)^4} \frac{M_1^{\text{loop}}(k_1', k_2', k_3, k_4)M_1(k_1, k_2, k_1', k_2')}{(k_1'^2 - \mu^2 + i\epsilon)(k_2'^2 - \mu^2 + i\epsilon)},$$

(4)

μ = pion mass,

where we use the following notation of the four-momenta:

$$k_1' = \tfrac{1}{2}P + q,$$

$$k_2' = \tfrac{1}{2}P - q,$$

$$P = k_1 + k_2$$

$$= k_3 + k_4,$$

$$P^2 = s$$

$$= W^2.$$

(5)

Performing a partial-wave expansion (dropping the isospin index),

$$M(k_i) = \sum_l (2l+1)P_l(\cos\theta_{13})M_l(k_i^2, s),$$

(6)

Eq. (4) reduces to

$$M_l(k_i^2, s) = M_l^{\text{loop}}(k_i^2, s)$$

$$-\frac{1}{4\pi^3 i} \int dq_0 \, |\vec{q}|^2 d|\vec{q}| \frac{M_l^{\text{loop}}(k_1'^2, k_2'^2, k_3^2, k_4^2, s)M_l(k_1^2, k_2^2, k_1'^2, k_2'^2, s)}{(k_1'^2 - \mu^2 + i\epsilon)(k_2'^2 - \mu^2 + i\epsilon)},$$

(7)

with

$$M_l^{\text{loop}}(k_i^2, s) = \tfrac{1}{2} \int_{-1}^{+1} d\cos\theta_{13} P_l(\cos\theta_{13})M^{\text{loop}}(k_i).$$

(8)

The normalization of the partial-wave amplitudes $M(k_i^2, s)$ is,[7] including the factor 2 for the $t \leftrightarrow u$ crossed diagrams,

$$M_l(k_i^2 = \mu^2, s) = -16\pi \left(\frac{s}{s-4\mu^2}\right)^{1/2} e^{i\delta_l} \sin\delta_l.$$

(9)

We now shall evaluate the kernel of the two-dimensional integral equation (7), which is given by Eqs. (2), (3), and (8), taking first the trace in (2). With the abbreviation $\pi_i \equiv P_i^2 - M^2$ we get

$$\text{tr}[(\not{P}_1 - M)(\not{P}_2 + M)(\not{P}_3 - M)(\not{P}_4 + M)]$$

$$= (\pi_1 + \pi_2 - k_1^2)(\pi_3 + \pi_4 - k_4^2)$$

$$+ (\pi_1 + \pi_4 - k_3^2)(\pi_2 + \pi_3 - k_2^2)$$

$$- (\pi_1 + \pi_3 - s)(\pi_2 + \pi_4 - t),$$

(10)

(a)   (b)   (c)
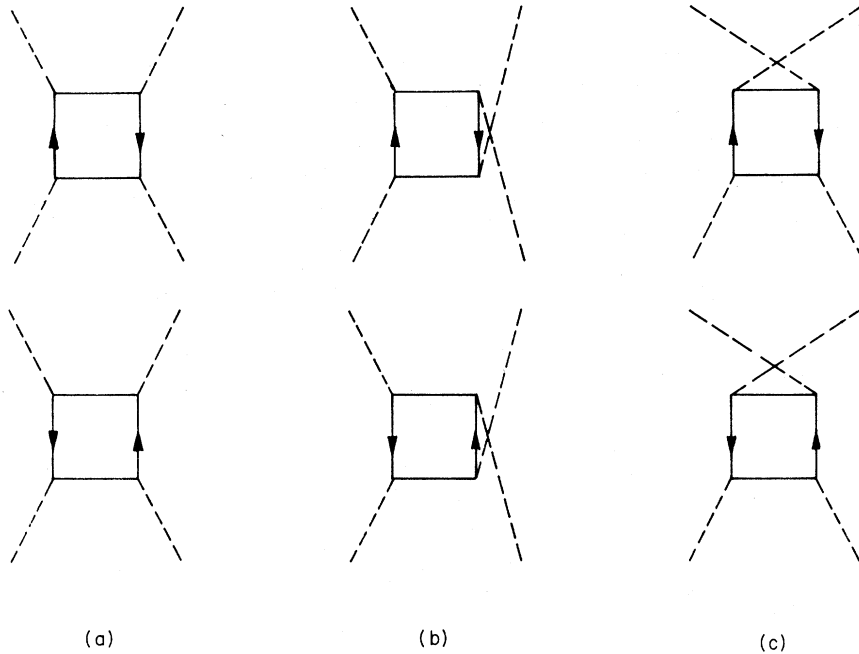
FIG. 3. (a)–(c) Complete set of fourth-order loop diagrams.

with $t = (k_1 - k_3)^2$. Here all the terms proportional to π_2 and π_4 can be dropped, since they only contribute to s waves. For moderate $k_i^2 \approx -M^2$, the last term in (10) with its factor t will dominate the p wave, since the denominators in (2) have little

variation with $\cos\theta_{13}$ because of the large nucleon mass. This corresponds to the standard picture of dominant s-wave intermediate $N\overline{N}$ states with parallel spin.

After expanding the propagators in (2) as

$$\pi_2^{-1}\pi_4^{-1} = \frac{1}{4\,|\vec{k}_1|\,|\vec{k}_3|\,|\vec{P}_1|^2} \sum_{l,l'} (2l+1)(2l'+1)P_l(\cos\theta(\vec{P}_1,\vec{k}_1))\,P_{l'}(\cos\theta(\vec{P}_1,\vec{k}_3))\,Q_l(z)Q_{l'}(z'),$$ (11)

with

$$z = \frac{M^2 - k_1^2 - P_1^2 + 2P_{10}k_{10}}{2\,|\vec{P}_1|\,|\vec{k}_1|},$$

$$z' = \frac{M^2 - k_3^2 - P_1^2 + 2P_{10}k_{30}}{2\,|\vec{P}_1|\,|\vec{k}_3|},$$

$Q_l(z) =$ Legendre function of the second kind, the integration (8) is easy, and we find, after performing a Wick rotation of the q_0 contour $(q_0 \to i\tau)$, for $l = 1$

$$M_1^{\text{loop}}(k_i^2, s) = -\left(\frac{g^2}{4\pi}\right)^2 \frac{32}{\pi} \int_{-\infty}^{+\infty} d\tau \int_0^\infty d|\vec{q}|\,|\vec{q}|^2 \frac{I(k_i^2, \tau, |\vec{q}|, s)}{(P_1^2 - M^2)(P_3^2 - M^2)},$$ (12)

with

$$P_{10} = \tfrac{1}{2}W + i\tau, \quad \vec{P}_1 = \vec{q}, \quad P_{30} = -\tfrac{1}{2}W + i\tau, \quad \vec{P}_3 = \vec{q},$$

and

$$I(k_i^2, \tau|\vec{q}|, s) = \frac{1}{4\,|\vec{k}_1|\,|\vec{k}_3|\,|\vec{q}|^2}((s - \pi_1 - \pi_3)\{(k_1^2 + k_3^2 - 2k_{10}k_{30})Q_1(z)Q_1(z')$$

$$+ \tfrac{2}{3}|\vec{k}_1|\,|\vec{k}_3|\,[Q_0(z)Q_0(z') + 2Q_2(z)Q_2(z')]\}$$

$$- [k_1^2k_4^2 + k_2^2k_3^2 + \pi_1\pi_3 - (k_1^2 + k_3^2)\pi_3 - (k_2^2 + k_4^2)\pi_1]Q_1(z)Q_1(z')).$$ (13)

In our following numerical calculations the terms proportional to $Q_2(z)Q_2(z')$ have been neglected, since $Q_2(z) \ll Q_0(z)$ for $z > 1.1$. The technical details of the numerical evaluation of the integrals in (12) and the subsequent solution of Eq. (7) will be described in the Appendix, and we turn to the results of these calculations.

III. THE $l = 1$ $\pi\pi$ PHASE SHIFT WITH CUTOFF IN THE NUCLEON LOOP

Since power counting for the kernel of (7), which apart from propagators and a factor $|\vec{q}|^2$ is given by (12), shows that it is not square integrable, we shall always work with a cutoff in all nucleon propagators, thereby avoiding also possible difficulties with the Wick rotation. As usual we shall make the substitution

$$\frac{1}{P_i^2 - M^2} \to \frac{1}{(P_i^2 - M^2)[1 - (P_i^2 - M^2)/\Lambda^2]},$$

$$i = 1, \ldots, 4. \quad (14)$$

We first consider the case of a very large cutoff

mass,

$$\Lambda^2 = 2 \times 10^4 M^2.$$

In this case an inspection of the first few terms of the perturbation expansion of $M(k_i^2, s)$ as given by Eq. (7) shows that the potential is about a factor of 50 too large compared to what is necessary to make the 2π state resonant at $s = m_\rho^2$. Quantitatively we obtain for a coupling constant

$$\frac{g^2}{4\pi} = 2.07$$

the $\pi\pi$ phase shift shown in Fig. 4 by a solid line (curve a). For comparison, the phase shift given by the relativistic Breit-Wigner formula for a p wave[8]

$$\frac{1}{W}\frac{|\vec{k}|^3}{|\vec{k}_\rho|^3}\cot\delta_1(W) = \frac{m_\rho^2 - s}{\Gamma_0 m_\rho^2},$$ (15)

$$|\vec{k}_\rho|^2 = \tfrac{1}{4}m_\rho^2 - \mu^2,$$

with $\Gamma_0 = 130$ MeV, is drawn in the same figure as curve c, and it is clear that the model phase cor-

responds to a very broad resonance ($\Gamma \sim 400$ MeV).

The width becomes even worse if we keep the coupling constant at its physical value and reduce the cutoff parameter until $\delta_1(m_\rho) = \frac{1}{2}\pi$. For

$$\Lambda^2 = 4.4M^2$$

and   (16)

$$\frac{g^2}{4\pi} = 14.5 \,,$$

we get the curve (b) shown in Fig. 4, which is hardly resonant, considering the trivial suppression of $\delta_1(W)$ at small W due to the p-wave threshold behavior.

We now can compare the value for Λ^2, Eq. (16), with the cutoff parameter in the nucleon propagators in the Δ case.[6] The $\Delta(1236)$ has been described as a resonating πN system in the framework of the BSE with one-nucleon exchange as the potential, so that the Δ mass depends also on the cutoff in the nucleon propagators. In the works cited in Ref. 6 a cutoff has been applied to the exchanged nucleons only, which led to $\Lambda_\Delta^2 = 4.6M^2$. Repeating the calculation, with the cutoff inserted into all nucleon propagators, gives us

$$\Lambda_\Delta^2 = 12M^2 \,,$$

in poor agreement with (16). Since in the ρ case the resonance width is strongly overestimated (in the Δ case the model phase shift is all right below the resonance but becomes increasingly worse as one passes through the resonance[6]), we conclude that this type of cutoff leads to too strong a suppression of the short-range part of the the $\pi\pi$ or πN potential. In Sec. IV we shall investigate the improvements that can be obtained from the inclusion of self-energy corrections as shown in Fig. 2.

IV. SELF-ENERGY CORRECTIONS

Generally the contributions from channels other than those considered above will hardly show any correlation between the Δ and the ρ problem. A connection exists, however, for the pion and nucleon self-energy diagrams like those of Fig. 2, and we can try to improve the consistency as well as the width problem by modifying the pion propagators in Eq. (7). In order to guide our ideas we first shall calculate these corrections in lowest-order perturbation theory. After mass and vertex renormalization we get for the pion propagator

$$\Delta'(k^2) = \frac{1}{k^2 - \mu^2} - \frac{g^2}{4\pi}\frac{2}{\pi}\int_{4M^2}^{\infty} ds \frac{s(1 - 4M^2/s)^{1/2}}{(s - k^2)(s - \mu^2)^2}$$

$$\approx \frac{1}{k^2 - \mu^2} - \frac{g^2}{4\pi}\frac{2}{\pi k^2}\left[1 - \frac{1}{2z}\ln\left(\frac{1+z}{1-z}\right)\right],$$

                      (17)

$$z = \left(\frac{-k^2}{4M^2 - k^2}\right)^{1/2},$$

where the pion mass has been neglected under the integral of (17). The "correction" term in (17)
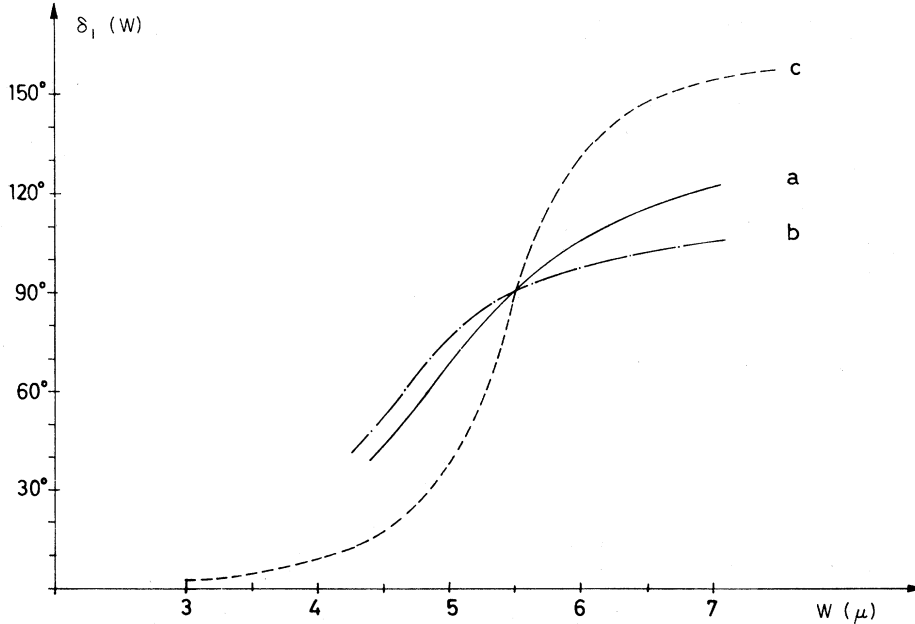
FIG. 4. $\pi\pi$ phase shift in the ρ channel: (a) large cutoff, $y^2/4\pi = 0.27$; (b) with cutoff $\Lambda^2 = 4.4 M^2$, $g^2/4\pi = 14.5$; (c) relativistic Breit-Wigner curve (Ref. 8) [Eq. (15)], $\Gamma_0 = 130$ MeV.

becomes equal to the bare propagator at k^2
$\approx -1.4M^2$. If we insert this propagator for the
bare ones in Eq. (7) and readjust Λ^2, we get the
$\pi\pi$ phase shown as a full line in Fig. 5, together
with the comparison phase (15), and we find Λ^2
$= 2.16M^2$. Although there is a considerable im-
provement beyond the phases (a) and (b) of Fig. 4,
the ρ width is still larger than the experimental
one by a factor of 2. In order to obtain better
agreement, it is necessary to multiply the correc-
tion term in (17) by 2, i.e., we set

$$\Delta'(k^2) = \frac{1}{k^2 - \mu^2} - \lambda \frac{g^2}{4\pi} \frac{2}{\pi k^2}\left[1 - \frac{1}{2z} \ln\left(\frac{1+z}{1-z}\right)\right]$$

(18)

and the resulting phase, for $\lambda = 2$, is shown as
curve (b) in Fig. 5.

It represents essentially a two-parameter fit to
the Breit-Wigner phase, where the fitting param-
eters are λ and

$$\Lambda^2 = 1.55M^2.$$

(19)

The physical significance of this result is that (a)
the value of λ is not too far off the perturbation-
theoretic value, and that (b) the value of Λ^2 is now
in reasonable agreement with the value

$$\Lambda_\Delta{}^2 = 2.15M^2,$$

(20)

which has been obtained after inserting the same
pion propagator modification into the ladders of the
$\Delta(1236)$ channel.

It is not very satisfactory that we have concen-
trated only on the pion-propagator modifications,
instead of also dealing with the $\pi N\bar{N}$ vertex as a
function of the pion four-momentum. There we
would expect a form-factor effect which may com-
pensate for the enhancement used in Eq. (18). But
one also should regard the possibility that the cut-
off mass for the nucleon propagators or vertices
depends on the pion four-momentum $k_i{}^2$. In view
of these difficulties the propagator modifications
(14) and (18) cannot be considered more than sim-
ple phenomenological parametrizations, leading to
approximate consistency in two physically very
different states.

V. CROSSING PROPERTIES

Our picture for the ρ meson as a mixture of $\pi\pi$,
$N\bar{N}$, and $2N\bar{N}$ states is only useful if the exchange
of multirung ladders in the t channel is relatively
unimportant, since this would lead to the presence
of more complicated multiparticle states in our ρ
"wave function". We can now, at least partially,
look into this question by calculating the p-wave
projection of the ladder series with nucleon loops
for negative energy squared in one channel (the t
channel, let us say) and performing its p-wave
projection into the crossed (s) channel. Then we
subtract from this ρ exchange the lowest-order
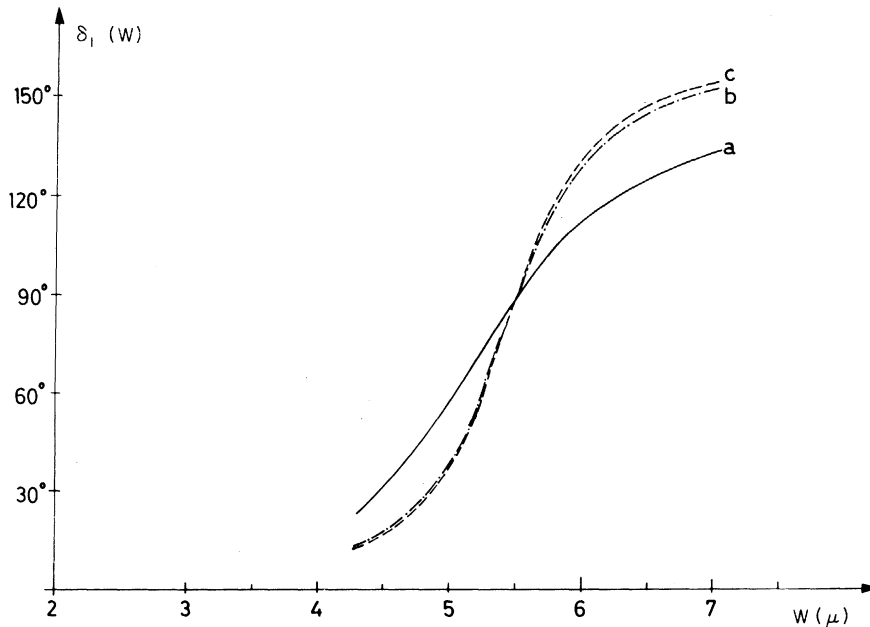
FIG. 5. $\pi\pi$ phase shift in the ρ channel: (a) self-energy contributions from perturbation theory, $\Lambda^2 = 2.16 M^2$; (b) twice the perturbation contribution for the self-energy, $\Lambda^2 = 1.55 M^2$; (c) relativistic Breit-Wigner curve (Ref. 8) (Eq. 15), $\Gamma_0 = 130$ MeV.

loop which has already been included correctly. It will turn out, for the most important pion off-shell four-momenta, that the diagrams with two or more nucleon loops in the t channel contribute little attraction into the s channel compared to the single loop.

From the partial-wave expansion of the invariant amplitude in the t channel,

$$M(k_i) = \sum_l (2l+1)P_l(z_t)M_l(k_i^2, t), \tag{21}$$

we find the ρ-exchange contribution to the s-channel p wave, which we call $M_{1,\rho}(k_i^2, s)$, by

$$M_{1,\rho}(k_i^2, s) = \tfrac{3}{4}\int_{-1}^{+1} dz_s z_s z_t M_1(k_i^2, t), \tag{22}$$

with

$$z_t = 1 + \frac{s}{2\vec{k}_t^2} \tag{23}$$

and

$$t = -2\vec{k}_s^2(1 - z_s). \tag{24}$$

The momenta $\vec{k}_t$ and $\vec{k}_s$ are the t- and s-channel c.m. three-momenta, respectively, which depend also on k_i^2, and we have specialized for convenience to the case of equal external masses k_i^2, $i = 1, \ldots, 4$. Equation (22) contains the $s \rightarrow t$ isospin crossing factor $\tfrac{1}{2}$.

We shall choose the value of k_i^2 according to where in the integrations in (7), after a transformation on a finite interval, the maximum of the integrand occurs. It is not surprising to find this maximum at relatively high four-momenta, namely

$$-q^2 \equiv \tau^2 + \vec{q}^2 \approx 3M^2.$$

Consequently we have evaluated Eq. (22) for $k_i^2 = -2M^2$. First we show in Fig. 6 the individual ladder diagrams for $M_1(k_i^2, t)$ in the t interval which is determined by (24), inserting $s = m_\rho^2$ and $k_i^2 = -2M^2$. One notices a strong decrease of all diagrams for large negative t, which is a consequence of the explicit energy dependence of the loop potential through the last term in (10) (where s is the energy variable). [The zero at $t = -8M^2$ is a consequence of the p-wave threshold behavior. It is compensated for by the pole in z_t, Eq. (23), at $|\vec{k}_t| = 0$.] Thus the potential becomes repulsive at $t \approx -4M^2$, and one observes the corresponding
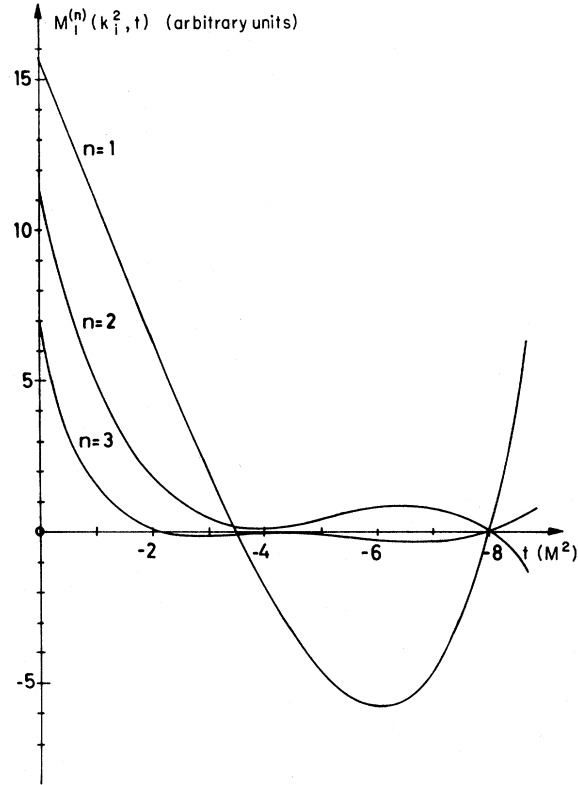
FIG. 6. Crossed-ladder p-wave contributions to the s-channel p wave at $s = m_\rho^2$. The number of loops in the t channel is denoted by n. The pion four-momenta are off shell.

alternation in sign of the higher-order ladder diagrams.

This zero of the potential does not occur for simple Yukawa-type potentials, so that the convergence of the ladder series may be worse than in our case. But if the potential is energy-independent, its range has to be much smaller in order to generate the narrow resonance, so that we have to consider the crossed ladders at still higher negative t. There the convergence may be as good as it is here.

Finally in Table I we list the result of the integration in Eq. (22) for the individual terms of the ladder series. The index n denotes the number of nucleon loops included ($n = 1 =$ box diagram). In the

TABLE I. s-channel partial-wave projections ($l = 1$) of t-channel p-wave ladder diagrams with n nucleon loops [see Eq. (22)]. The last column is the full p-wave projection of the nucleon loop. All amplitudes have virtual pion masses $k_i^2 = -2M^2$. Units are arbitrary.

n	1	2	3	4	5	6	$M_1^{\text{loop}}(k_i^2 = -2M^2, m_\rho^2)$
$M_{1\rho}^{(n)}(k_i^2 = -2M^2, m_\rho^2)$	1.73	0.316	0.244	0.070	0.099	0.003	4.78

last column the direct-channel p-wave projection of the box diagram for the same k_i^2 is listed, and it is seen that the "truncated ρ exchange" (i.e., ρ exchange minus box) is a 10% correction to the dominant box potential. Whether a similar statement can be made with respect to the crossed s waves requires more calculations.

VI. SUMMARY AND DISCUSSION

A composite model has been presented for the ρ meson where the constitutents are $\pi\pi$, $N\overline{N}$, and $2N\overline{N}$, the latter being coupled through self-energy effects. Only the nondiagonal coupling given by one-nucleon exchange has been kept as a force, and a suppression of the short-range parts via a phenomenological cutoff was necessary for understanding the ρ mass, and the self-energy effects had to be made stronger by a factor of 2 than their perturbation-theoretic value for fitting the ρ width properly. The consistency of the cutoff parameter with that of the $\Delta(1236)$ case is reasonable which allows the possibility that our forces are not completely ad hoc.

Within this model ρ exchange as a force between the pions is, after subtraction of the crossing symmetric box diagram, at short distances (of the order of $1/M$) only a minor correction to the dominant nucleon box. This is in analogy to the results of bootstrap calculations, where only a very broad ρ meson can provide enough attraction.[1] From this fact the conclusion that $N\overline{N}$ states are very important for a description of the ρ has been drawn repeatedly.[9]

Apart from possible changes in the potential by Δ exchange, etc., two major open problems are very important:

(a) The SU(3) structure, like the absence of exotic states, has to be explained. For this it is necessary to consider crossed diagrams like those of Fig. 2 which contribute to the exotic $I = 2$ channel. Since they do not have an absorptive part in the s channel, they are not necessarily attractive.
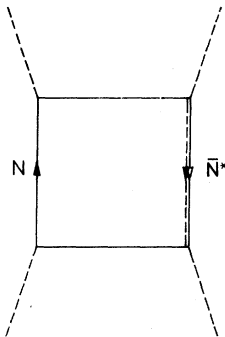
FIG. 7. $N\overline{N}^*$ contribution to higher-spin $\pi\pi$ amplitudes.

(b) It is unlikely that the nucleon loop as a very short-range force can explain the existence of higher-spin resonances like the f or g meson. The most straightforward explanation[10,11] is probably the inclusion of higher-spin baryon resonances like $\Delta(1236)$ and $N^*(1525)$ $(=D_{13})$, etc., into the baryon loop. It is natural to expect from Fig. 7, after taking the spin trace, a factor t^2 entering the kernel $K(k_i)$, if N^* is a spin-$\frac{3}{2}$, negative-parity particle, so that a large projection into $J^P = 2^+$ two-pion states should occur. Whether we can understand in this way the similarity between the meson and baryon Regge slopes remains to be seen.

APPENDIX

We want to describe our numerical methods of solving the Bethe-Salpeter equation (BSE), Eq. (7), with the kernel (12).

The BSE has been iterated numerically, so that formally

$$M_1(k_i^2, s) = \sum_{n=1} g^{4n} M_1^{(n)}(k_i^2, s). \tag{A1}$$

From the expansion coefficients $M_1^{(n)}(k_i^2 = \mu^2, s)$ the diagonal Padé approximants[12] $[M_1]_{N,N}$ have been formed, which are determined by the requirement that with two polynomials $P_N(x)$ and $Q_N(x)$ of order N, the power-series expansion of

$$[M_1]_{N,N} = \frac{P_N(x)}{Q_N(x)}, \qquad x = g^4 \tag{A2}$$

with respect to x agrees with (A1) up to $n = 2N$. Good numerical convergence has been observed for $N \geq 2$, whereas the $N = 1$ approximant generally overestimates the attraction. [This is in contrast to the $\Delta(1236)$ case.[13]]

The main problem remains to compute the kernel as the two-dimensional integral (12) for a number of values of the k_i^2, and to perform the integrations in (7), both with a minimum number of mesh

points. For the integrations, a generalized Gaussian quadrature has been used which will be described briefly in the following.

If we want to integrate

$$\int_a^b dx\, f(x) \quad \text{with} \quad f(x) = P_{2N-1}(x) w(x), \qquad (A3)$$

where $P_{2N-1}(x)$ is a polynomial of order $2N-1$, and the weight function $w(x)$ is nonnegative in $a \leqslant x \leqslant b$, then it is possible to find points x_n with $a \leqslant x_n \leqslant b$ and weights h_n such that[14]

$$\int_a^b dx\, f(x) = \sum_{n=1}^N h_n f(x_n). \qquad (A4)$$

The x_n can be found as the roots of the following polynomial:

$$Q_N(x) = \sum_{n=0}^N c_n x^n, \qquad (A5)$$

where the coefficients c_n are determined by the N linear equations

$$\int_a^b dx\, w(x) Q_N(x) x^m = \int_a^b dx\, w(x) \sum_{n=0}^N c_n x^{m+n}$$

$$= 0,$$

$$m = 0, \dots, N-1 \qquad (A6)$$

and by

$$c_N = 1.$$

The weights h_n are given through the N linear equations

$$\sum_{n=1}^N h_n x_n^m w(x_n) = \int_a^b dx\, w(x) x^m,$$

$$m = 0, \dots, N-1. \qquad (A7)$$

In practice we first compute the moments $\int_a^b dx\, w(x) x^m$ by a standard Gaussian quadrature using some 100 points, then solve (A6) for the c_n, find the roots of (A5), and finally solve (A7) for the h_n.

We have listed the above well-known formulas because they can be immediately extended to the case of a principal-value integral, which occurs in the $|\vec{q}|$ integration of (7) through the mass-shell singularities. Consider the integral

$$P \int_a^b dx\, \frac{f(x)}{x-y} = P \int_a^b dx\, \frac{P_{2N-1}(x) w(x)}{x-y}, \qquad (A8)$$

with the same conditions on $w(x)$ and $P_{2N-1}(x)$ as above. Assume we calculated the coefficients c_n and the roots x_n as in (A6) and (A5), i.e., disregarding for a moment the denominator $x-y$ in (A8). Then we define

$$x_{N+1} = y, \qquad (A9)$$

and solve

$$\sum_{n=1}^{N+1} k_n x_n^m w(x_n) = P \int_a^b dx\, \frac{w(x) x^m}{x-y},$$

$$m = 0, \dots, N \qquad (A10)$$

for the h_n, where the right-hand sides of (A10) are again evaluated numerically with many points (using some tricks to make the singular point $x = y$ harmless). Then we claim that

$$P \int_a^b dx\, \frac{f(x)}{x-y} = \sum_{n=1}^{N+1} h_n f(x_n), \qquad (A11)$$

if $f(x)$ is of the form indicated in (A8). This can be understood easily, because with

$$Q'_{N+1}(x) = Q_N(x)(x-y), \qquad (A12)$$

Eq. (A6) is identical with

$$P \int_a^b dx\, \frac{x^m}{x-y} w(x) Q'_{N+1}(x) = 0,$$

$$m = 0, \dots, N-1. \qquad (A13)$$

Any polynomial of degree $2N-1$ can be written as

$$P_{2N-1}(x) = Q'_{N+1}(x) q_{N-2}(x) + r_N(x), \qquad (A14)$$

where $q_{N-2}(x)$ and $r_N(x)$ are again polynomials. Now the integral of the first term in (A14) vanishes because of (A13), and its contribution on the right-hand side of (A11) is zero because the x_n are the roots of Q'_{N+1}. The second term in (A14) is integrated exactly through (A11) because of (A10), which completes the proof.

In the remaining part we have to discuss our choices of the weight functions $w(x)$ for the various integrations. First of all the two-dimensional integrations in (7) and (12) are transformed into polar coordinates:

$$\int_{-\infty}^{+\infty} d\tau \int_0^\infty d|\vec{q}|\, |\vec{q}|^2 = \int_0^\infty dq\, q^3 \int_{-1}^{+1} d\cos\alpha \sin\alpha, \qquad (A15)$$

with

$$q_0 = i\tau$$

$$= iq\cos\alpha$$

and

$$|\vec{q}| = q\sin\alpha.$$

While in (12) the $d\cos\alpha$ integration is straightforward, one encounters in (7) the well-known propagator poles in $\cos\alpha$, which have been handled by numerical subtraction and analytical addition. Since in (12) $N\bar{N}$ s waves are dominant, there are no threshold factors in $|\vec{q}|$ so that the weight function is simply

$$w_\alpha(\cos\alpha) = \sin\alpha, \qquad (A16)$$

whereas for (7) the p-wave threshold factors allow for

$$w'_\alpha(\cos\alpha) = \sin^3\alpha. \qquad (A17)$$

For the dq integrations we took essentially the integrand of a box diagram. Thus for (12) we choose

$$w(q) = \int_{-1}^{+1} d\cos\alpha \, \frac{qQ_0^2(z)}{\sin\alpha(P_1^2 - M^2)(P_3^2 - M^2)},$$

$$(P_{10}, |\vec{P}_1|) = (\tfrac{1}{2}W + iq\cos\alpha, q\sin\alpha),$$

$$(P_{30}, |\vec{P}_3|) = (\tfrac{1}{2}W - iq\cos\alpha, q\sin\alpha), \qquad (A18)$$

$$z = \frac{q^2 + \vec{k}^2 + M^2}{2|\vec{P}_1||\vec{k}|},$$

$$\vec{k}^2 = \tfrac{1}{4}s - \mu^2.$$

For (7), which is a principal-value integral in q, we took

$$w'(q) = \oint_{-1}^{+1} d\cos\alpha \, \frac{qQ_1^2(z')(x - y)}{\sin\alpha(k_1^2 - \mu^2 + i\epsilon)(k_3^2 - \mu^2 + i\epsilon)}, \qquad (A19)$$

where

$$x = \frac{-a + q}{a + q},$$

$$y = \frac{-a + |\vec{k}|}{a + |\vec{k}|},$$

$$(k_{10}, |\vec{k}_1|) = (\tfrac{1}{2}W + iq\cos\alpha, q\sin\alpha),$$

$$(k_{20}, |\vec{k}_2|) = (\tfrac{1}{2}W - iq\cos\alpha, q\sin\alpha),$$

$$z' = \frac{q^2 + \vec{k}^2 + 4M^2}{2|\vec{k}_1||\vec{k}|},$$

$$a \approx 10\mu.$$

The symbol $\oint$ denotes that the path of integration encircles the propagator poles properly.

The factor $(x - y)$ in (A19) cancels the pole coming from the propagators, and it is reintroduced by using the integration technique described after Eq. (A8). Unless the extra point y coincides very closely with one of the mesh points x_n, $n = 1, \ldots, N$, the integrations can be done with reasonable accuracy ($\sim 5\%$) with $N = 4$ only. The reported calculations are based on $N = 7$.

*This work was supported in part by the U. S. Atomic Energy Commission, Contract No. AT(11-1)-1764.

[1]See the two reviews: J. L. Basdevant and J. Reignier, in *Proceedings of the International School of Elementary Particle Physics at Herceg-Novi, Yugoslavia, 1970* (Secretariat du Département de Physique Corpusculaire, Centre de Recherches Nucléaires, Strasbourg-Cronenbourg, France, 1970); P. D. B. Collins and E. J. Squires, *Regge Poles in Particle Physics* (Springer, Berlin, 1968). See also B. R. Webber, Phys. Rev. D **3**, 1971 (1971) and references quoted therein.

[2]J. J. J. Kokkedee, *The Quark Model* (Benjamin, New York, 1969); P. Narayanaswamy and A. Pagnamenta, Nuovo Cimento **53A**, 635 (1968); M. Böhm, H. Joos, and M. Krammer, Nuovo Cimento **7A**, 21 (1972); DESY Report No. 72/11, 1972 (unpublished); M. K. Sundaresan and P. J. S. Watson, Ann. Phys. (N.Y.) **71**, 443 (1972).

[3]E. Fermi and C. N. Yang, Phys. Rev. **76**, 1739 (1949); G. L. Kane and W. F. Palmer, *ibid.* **172**, 1648 (1968); H. Sugawara and F. von Hippel, *ibid.* **172**, 1764 (1968); *ibid.* **185**, 2064 (1969); G. Patergnani, Z. Physik **232**, 223 (1970); G. Schierholz and S. Wagner, Nucl. Phys. **B32**, 306 (1971).

[4]N. Nakanishi, Progr. Theoret. Phys. (Kyoto) Suppl.

43, 1 (1969).

[5]K. D. Rothe, Phys. Rev. **170**, 1548 (1968).

[6]J. A. Tjon and H. M. Nieland, in *The Padé Approximant in Theoretical Physics*, edited by G. Baker, Jr. and J. L. Gammel (Academic, New York, 1970); F. Gutbrod, DESY Report No. 69/33, 1969 (unpublished).

[7]J. D. Bjorken and S. D. Drell, *Relativistic Quantum Fields* (McGraw-Hill, New York, 1965).

[8]J. D. Jackson, Nuovo Cimento **34**, 1644 (1964).

[9]J. S. Ball and M. Parkinson, Phys. Rev. **162**, 1509 (1967).

[10]S. Mandelstam, Phys. Rev. **166**, 1539 (1968).

[11]P. Carruthers and M. M. Nieto, Phys. Rev. Letters **18**, 297 (1967); **163**, 1646 (1967).

[12]See the two reviews: J. Zinn-Justin, Phys. Reports **1C**, 55 (1971); G. A. Baker, Advan. in Theoret. Phys. **1**, 1 (1965).

[13]H. A. Nieland and J. A. Tjon, Phys. Letters **27B**, 309 (1968).

[14]See any book on numerical integration, e.g., I. S. Berezin and N. P. Zhidkov, *Computing Methods* (Pergamon, Oxford, 1965).